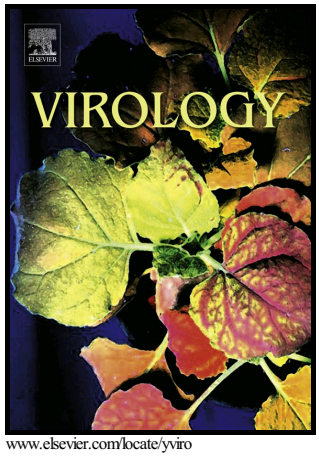

www.elsevier.com/locate/yviro

eEF1A demonstrates paralog specific effects on HIV-1 reverse transcription efficiency

Dongsheng Li, Daniel J. Rawle, Zhonglan Wu, Hongping Jin, Min-Hsuan Lin, Mary Lor, Catherine M. Abbott, David Harrich

PII: S0042-6822(19)30027-3
DOI: https://doi.org/10.1016/j.virol.2019.01.023
Reference: YVIRO9015

To appear in: *Virology*

Received date: 26 November 2018
Revised date: 25 January 2019
Accepted date: 28 January 2019

Cite this article as: Dongsheng Li, Daniel J. Rawle, Zhonglan Wu, Hongping Jin, Min-Hsuan Lin, Mary Lor, Catherine M. Abbott and David Harrich, eEF1A demonstrates paralog specific effects on HIV-1 reverse transcription efficiency, *Virology,* https://doi.org/10.1016/j.virol.2019.01.023

eEF1A demonstrates paralog specific effects on HIV-1 reverse transcription efficiency

Dongsheng Li[a], Daniel J. Rawle[a,b], Zhonglan Wu[c], Hongping Jin[a], Min-Hsuan Lin[a], Mary Lor[a], Catherine M. Abbott[d] and David Harrich[a*]

a. Department of Cell and Molecular Biology[1] and Department of Genetics and Computational Biology[2], QIMR Berghofer Medical Research Institute, Herston, Qld, 4006, Australia
b. School of Chemistry and Molecular Biosciences, University of Queensland, St. Lucia, Qld, 4072, Australia
c. Ningxia Center for Disease Control and Prevention, Ningxia, 750001, China
d. Medical Genetics Section, Centre for Genomic and Experimental Medicine, Institute of Genetics and Molecular Medicine, Western General Hospital, University of Edinburgh, Edinburgh, United Kingdom

*Correspondence: Department of Cell & Molecular Biology, QIMR Berghofer Medical Research Institute, 300 Herston Rd, Herston, QLD,4006, Australia david.harrich@qimrberghofer.edu.au

ABSTRACT

The eukaryotic translation elongation factor 1A (eEF1A) has two cell-type specific paralogs, eEF1A1 and eEF1A2. Both paralogs undertake a canonical function in delivering aminoacyl-tRNA to the ribosome for translation, but differences in other functions are emerging. eEF1A1 has been reported to be important for the replication of many viruses, but no study has specifically linked the eEF1A2 paralog. We have previously demonstrated that eEF1A1 directly interacts with HIV-1 RT and supports efficient reverse transcription. Here, we showed that RT interacted more strongly with eEF1A1 than with eEF1A2 in immunoprecipitation assay. Biolayer interferometry using eEF1A

paralogs showed different association and dissociation rates with RT. Over expressed eEF1A1, but not eEF1A2, was able to restore HIV-1 reverse transcription efficiency in HEK293T cells with endogenous eEF1A knocked-down and HIV-1 reverse transcription efficiency correlated with the level of eEF1A1 mRNA, but not to eEF1A2 mRNA in both HEK293T and primary human skeletal muscle cells.

Keywords: HIV-1, eEF1A, paralog, replication, reverses transcription, human primary skeletal muscle cell, HEK 293T cell

1. Introduction

The eukaryotic translation elongation factor 1A (eEF1A) is a highly abundant cellular protein involved in delivering aminoacyl-tRNAs to ribosomes for polypeptide synthesis. It is encoded by two single copy gene paralogs, EEF1A1 and EEF1A2, located on chromosomes 6q13 and 20q13.33 respectively. EEF1A1 and EEF1A2 are present in all vertebrates. The amino acid sequence of the two human eEF1A paralogs, eEF1A1 (A1) and eEF1A2 (A2), have 92% identity and 98% similarity, but the paralogs are differentially expressed in certain cell types. A2 is expressed in terminally differentiated muscle, heart, neuronal tissue and in some specialized cells of pancreatic islet and gut tissues, whereas A1 is expressed in all other cell types (Soares and Abbott, 2013). The differential expression of eEF1A paralogs is regulated during embryogenesis where A1 is initially expressed but its expression is replaced by A2 in the cell types described above once terminal differentiation is achieved. In addition to the canonical role in protein synthesis, eEF1A1 has a growing list of additional, but sometimes interlinked functions, including protein degradation (Gonen et al., 1994;

Hotokezaka et al., 2002), cellular apoptosis (Chang and Wang, 2007; Ruest et al., 2002), nucleocytoplasmic trafficking (Khacho et al., 2008; Kohler and Hurt, 2007; Murthi et al., 2010), heat shock responses (Shamovsky et al., 2006), and multiple aspects of cytoskeletal regulation (Kim and Coulombe, 2010), highlighting its importance in diverse cellular processes (Mateyak and Kinzy, 2010). While previous functional studies of eEF1A focused primarily on the A1 paralog, emerging data shows that the A2 paralog has distinct functions to A1 (Hotokezaka et al., 2002; Novosylna et al., 2017; Soares and Abbott, 2013; Soares et al., 2009). For example, the appearance of A2 in the tissue where it is not normally expressed is thought to be related to tumour development (Abbas et al., 2015; Hassan et al., 2018). Another example is where A1 but not A2 plays a regulatory role in heat shock response (Vera et al., 2014).

eEF1A is reported to be involved in the replication of several viruses by distinct mechanisms. Accumulating reports indicated that eEF1A can interact with HIV-1 Gag, integrase, Nef and RT proteins, as well as HIV-1 genomic RNA to perform multiple roles in HIV-1 replication (Abbas et al., 2012; Li et al., 2013; Li et al., 2015a). eEF1A was detected in purified HIV particles, but not murine leukaemia virus (MLV) particles, suggesting that eEF1A is incorporated specifically into HIV particles and this incorporation is dependent on HIV Gag and RNA (Cimarelli and Luban, 1999). Recently we showed that eEF1A also binds to HIV-1 genomic RNA and was important for reverse transcription (Li et al., 2015a). Since most primary cells and cell lines used for these virus infection studies express exclusively or predominately A1, the reported functions of eEF1A in virus replication is presumed to be the A1 paralog (Li et al., 2013; Nagy, 2015), even though many immortal cell lines also express varying levels of A2. It is unknown if A2, like A1, functions in the replication of viruses. It remains an important and interesting question whether the cell type specific expression of certain eEF1A paralogs can explain differences in virus cytotropism for different cells in the body. Whether A1, A2 or other cellular factors play roles in the cytotropism and productive verse non-productive HIV-1 infection is an unanswered question (Bissel and Wiley, 2004).

We have demonstrated that eEF1A can interact with HIV-1 reverse transcriptase (RT) and is incorporated in reverse transcription complexes (RTCs) in HEK293T and Jurkat $CD4^+$ T cells, both of which express predominantly eEF1A1 (Warren et al., 2012). We have previously shown that this interaction has important roles in HIV-1 reverse transcription and replication (Li et al., 2015b; Rawle et al., 2018; Warren et al., 2012). While a role for eEF1A in reverse transcription may be facilitated by interactions in virions, proposed and experimentally supported models of uncoating suggest the viral core, a capsular structure composed of capsid protein, becomes "leaky" after 30 minutes (Francis and Melikyan, 2018; Mamede et al., 2017), which could also enable RTC interaction with cytoplasmic pools of eEF1A and completion of reverse transcription.

The current study compared the interaction of HIV-1 RT with the two eEF1A paralogs and investigated effects of their overexpression or knockdown in HIV-1 reverse transcription. The eEF1A1 paralog maintained a tighter interaction with HIV-1 RT, and efficiency of reverse transcription correlated with the level of A1, but not A2, in both the human HEK293T cell line and the human primary skeletal muscle cells, suggesting that A1 is the major regulator of HIV reverse transcription.

2. Results

2.1. HIV-1 RT interacts with eEF1A1 tighter than eEF1A2 in HEK293T cells. Previously we reported that HIV-1 RT and endogenous eEF1A can be co-immunoprecipitated (co-IP) by an anti-eEF1A antibody from cell lysates (Li et al., 2015b). To examine whether A2 is also able to bind to RT, a co-IP assay was used. A1 or A2, which were each C-terminally FLAG-tagged, were individually co-expressed with V5 epitope tagged HIV-1RT p51 subunit in HEK293T cells. Western blot showed that the levels of RT were similar in all cell lysates tested (Figure 1A), and FLAG-tagged A1 and A2 were expressed similarly (Figure 1B). Cell lysates were prepared for co-IP reactions using a rabbit anti-FLAG antibody. The level of RT in the co-IP product was determined

by western blot using a mouse anti-V5 antibody. Western blot of these co-IP reactions showed a significantly decreased association of RT with A2 compared to A1 (Figure 1D and 1F), even though more A2-FLAG was present in the co-IP than A1-FLAG (Figure 1E). The results indicate that, like A1, A2 can bind to RT, albeit at a substantially lower level.

2.2. Purified eEF1A1 and eEF1A2 proteins from mouse tissues show distinct profiles of RT binding in biolayer interferometry (BLI) assays. The overexpression of A1 and A2 in HEK293T cells occurs in a background of endogenous eEF1A protein, predominantly the A1 paralog. To overcome eEF1A paralog co-expression that could complicate binding kinetic analysis of eEF1A to RT, cellular A1 and A2 proteins were purified from adult mouse liver that only expresses A1, and adult mouse skeletal muscle that only expresses A2 (Yaremchuk et al., 2012). Mouse and human eEF1A1 and 1A2 are almost identical, however it has a single amino acid difference between species for both paralogs. The purified protein underwent SDS-PAGE and was stained with Coomassie brilliant blue reagent. A 50 kDa protein corresponding to the molecular mass of eEF1A was detected (Figure 2A), and was identified by western blot using a goat anti-eEF1A antibody, which detects both paralogs, and an A2 specific anti-eEF1A antibody as shown (Figure 2B).

Since there is no specific subtype antibody for eEF1A1, we used RT-qPCR to specifically measure the level of A1 and A2 mRNA in the tissues as a way to gauge relative expression of each paralog. The primers from different regions of A1 and A2 mRNA were compared and one set of primers that gave the best sensitivity and specificity of detection for A1 and A2 were selected (Supplementary Table 1). Total RNA was extracted from mouse liver and skeletal muscle tissues and the level of A1 and A2 mRNA were determined using RT-qPCR. The result showed that A1 mRNA (Soares and Abbott, 2013) is dominant in liver tissue and A2 mRNA is dominant in skeletal muscle (Figure 2C).

The binding kinetics of HIV-1 RT with purified A1 and A2 was determined by biolayer interferometry (BLI) assays using the Octet system as described previously (Li et al., 2015b). In this assay, the RT heterodimer was biotinylated and bound to a streptavidin-coated biosensor. The interaction of RT with cellular A1 or A2 was examined by immersion of the biosensor into solutions containing 90 nM, 30 nM and 10 nM of each protein (Figure 2D). The analysis of three independent experiments shown in table 1 measured an association rate (k_a) of A2 and RT that rapidly reached a plateau, and which exceeded the k_a of A1 and RT by 3-fold. However the dissociation rate (k_d) of A2 and RT was ~6-fold higher than the k_d of A1 and RT. During the dissociation phase, the binding of A1 and RT was measurably higher than A2 and RT at every protein concentration tested. Hence although the affinity constants are somewhat similar, where both have very strong low nm K_D values, the data confirm increased stability of the RT:eEF1A1 complex compared to RT:eEF1A2 complex.

Table 1. Association and dissociation parameters of eEF1A1 and eEF1A2 with RT in BLI assay

protein	k_a (1/MS) (1)	k_d (1/second) (2)	K_D (nM) (3)	χ^2 (4)
eEF1A1	$9.60 \pm 3.54\times10^{4}$	$1.05 \pm 0.11\times10^{-4}$	1.23 ± 0.55	1.29 ± 1.16
eEF1A2	$2.91 \pm 0.41\times10^{5}$	$6.55 \pm 0.33\times10^{-4}$	2.31 ± 0.41	6.09 ± 2.03

(1) association rate constants (k_a): The rate of complex formed per second in a 1 molar solution of each component.
(2) dissociation rate constant (k_d): Stability of the complex, i.e. the fraction of complex decays per second.
(3) affinity constant (K_D): $K_D = k_d/k_a$. Significant difference between eEF1A1 and eEF1A2 ($p<0.05$)
(4) chi-square test: the goodness of curve fit, where below 10 is considered acceptable (Herschhorn et al., 2008) .

2.3. Exogenously overexpressed eEF1A1, but not eEF1A2, restores HIV-1 reverse transcription efficiency in cells with endogenous eEF1A1 downregulated. We had previously demonstrated that knockdown of endogenous A1 in HEK293T cells by siRNA treatment impaired HIV-1 reverse transcription efficiency (Warren et al., 2012). Since the A2 paralog co-immunoprecipitated with RT less than the A1 paralog, we performed experiments to examine whether exogenous overexpression of A1 and A2 could restore HIV-1 reverse transcription efficiency in cells where levels of

endogenous A1 were downregulated in HEK293T cells. The nucleotide sequence of an A1 cDNA was mutated to use alternative codons that would make the transcribed mRNA resistant to the A1 siRNA used in the experiments (ResA1). ResA1 or A2 were C-terminally fused in frame with mCherry (mCh) via a T2A ribosomal skipping sequence making mCh-T2A-ResA1 and mCh-T2A-A2 (Figure 3A). The T2A sequence allows for independent translation of eEF1A and mCherry.

HEK293T stable cell lines expressing exogenous ResA1 or A2 were obtained by transduction with a lentiviral vector and purified by FACS sorting for mCherry expression. Non-transduced HEK293T cells and stable cell lines expressing exogenous ResA1 or A2 were treated with a siRNA targeting endogenous eEF1A1 ($siRNA_{A1}$), or with a non-specific control siRNA ($siRNA_C$), and then infected using HIV-$1_{pNL4\text{-}3.Luc.R\text{-}E\text{-}}$ pseudotyped with VSV-G. The virus infections were synchronised for entry and each infection was continued for 4 h and then cell lysates were made. The level of total eEF1A protein in each lysate was measured by western blot (Figure 3B). The levels of β-tubulin in each sample indicated that the amount of lysate used were similar (Figure 3B, bottom panel). ImageJ software (Schneider et al., 2012) was used to measure the level of eEF1A in each lane relative to the cell only sample (Figure 3, lane 1), with each value normalized to levels of β-tubulin in that sample. The amount of A1 in cell lysate decreased by ~80% in cells treated with $siRNA_{A1}$ compared to the control $siRNA_C$ (Figure 3B, lane 1 vs. lane 4). However, the levels of exogenous overexpressed ResA1 and A2 were not affected by either siRNA treatment (Figure 3, lanes 2 and 3 vs. 5 and 6), and more eEF1A protein was detected in those cell lysates compared to the cell only control (Figure 3B, lane 1).

The levels of HIV-1 reverse transcription products in the cell lysates were measured by qPCR including the early DNA (negative strand strong stop DNA) (Figure 3C), and the late DNA (second strand transfer DNA) (Figure 3D). All qPCR measurements were normalized to cytochrome c oxidase subunit II DNA levels in each sample. The reverse transcription efficiency refers to the ratio of late DNA to early DNA (Figure 3D). The knockdown of endogenous A1 in HEK293T cells with

$siRNA_{A1}$ resulted in a modest change in early DNA level in HEK293T cells (Figure 3C), although the difference was not statistically significant. The level of late DNA was significantly lower when cells were treated with $siRNA_{A1}$ compared to $siRNA_c$ (Figure 3D), as observed previously (Warren et al., 2012). Levels of late DNA were restored by overexpression of exogenous Res-A1 (Figure 3D). A small increase in late DNA levels was observed when A2 was overexpressed, but this was not statistically significant (Figure 3D). Finally, the reverse transcription efficiencies, which is the percentage of late DNA copies to early DNA copies, showed a similar pattern to the late DNA levels (Figure 3E), where $siRNA_{A1}$ inhibited reverse transcription efficiency, which was significantly increased when Res-A1 was overexpressed, and not significantly increased by eEF1A2 overexpression. The results suggest that the more stable interaction of the A1 paralog with RT improves reverse transcription, as only Res-A1 could restore HIV late DNA synthesis in cells in a statistically significant manner when A1 levels were downregulated by $siRNA_{A1}$.

Total RNA was extracted from the siRNA treated and HIV infected HEK 293T cells and reverse transcribed to cDNA using random primers followed by specific measurement of eEF1A1 and A2 mRNA using qPCR. The GAPDH mRNA was also measured and used as an internal control. The relative level of A1 mRNA was 30 fold higher than A2 in HEK293T cells (Figure 4). A1 siRNA treatment reduced A1 mRNA levels by 83%, which was similar to the measured decrease in A1 protein levels (Figure 3B). The correlation analysis of A1 or A2 mRNA levels with the efficiency of HIV-1 reverse transcription showed that the level of A1 is correlated with reverse transcription efficiency (r^2=0.655, Figure 4A), but A2 is not (r^2=0.059, Figure 4B). These results confirmed the finding at the mRNA level that A1, not A2 is crucial for efficient HIV reverse transcription.

2.4. Primary human skeletal muscle cells (SKMC) express dominantly A1, not A2 when the cells were cultured in the growth medium and differentiated to myotubes. The results from HEK293T cells demonstrated that the level of A1, not A2 protein is important for HIV-1 reverse

transcription. We planned to test this finding in an A2 paralog dominant cellular environment. Since skeletal muscle cells are reported to express only A2, we explored a primary human skeletal muscle cell (SKMC) culture system to examine the effect of A2 on HIV-1 reverse transcription. The cells were cultured in SKMC growth medium following the product protocol. The cellular RNA was extracted when the cell confluence reached 70% at day 4 and 90% at day 5 of culture followed by RT-qPCR to determine the level of A1 and A2. Surprisingly, similar to HEK293T cell line, the relative level of A1 is substantially higher than A2 in SKMCs (Table 2).

Table 2. Relative levels of A1 and A2 in SKMCs and differentiated myotubes

	4 days of culture		5 days of culture	
	Growth medium	Differentiation medium	Growth medium	Differentiation medium
A1/GAPDH[1]	2.1979±0.1155	5.9835±0.1287	2.07±0.1234	5.3172±0.1178
A2/GAPDH[1]	0.0014±0.0001	0.0259±0.0033	0.0014±0.0001	0.0245±0.0011
A1/A2[2]	1592.96±69.926	232.9±22.174	1487.15±105.553	216.97±7.41

1. Ratio of A1 or A2 mRNA copy number/GAPDH mRNA copy number.
2. Ratio of the relative level of A1/A2

A previous study showed that the mouse and rat derived skeletal myoblast cell lines can differentiate into multinucleated myotubes *in vitro*, which results in increasing level of A2 and decreasing level of A1 (Ruest et al., 2002). Therefore we differentiated the primary human SKMCs to myotubes by replacing SKMC growth medium when the cells reached 50% confluence with fusion medium following the manufacturer instructions. At day 4 and 5 post-differentiation, the multinucleated myotubes were formed and the cellular RNA was extracted to examine the relative levels A1 and A2 mRNA by RT-qPCR. The results showed that relative levels of A2 mRNA (relative to GAPDH mRNA) increased around 20 fold (Table 2) at day 4 or day 5 of differentiation. Compared with the cells cultured in growth medium, the ratios of A1/A2 mRNA dropped from 1373~1554 to 214~229. The experiment revealed that A1 paralog is dominant in SKMCs, even after they differentiate to myotubes *in vitro*, and therefore myotubes were not used in further experiments.

2.5. HIV-1 reverse transcription efficiency is also correlated with the level of A1, not A2 in SKMCs. Even though SKMCs still predominantly expressed the A1 paralog, we determined the reverse transcription efficiency and infectivity in these cells to confirm the results in a primary cell that has not been previously used to investigate HIV-1 reverse transcription efficiency. To determine the HIV-1 reverse transcription efficiency in SKMCs, cells were transduced with the same lentiviral vectors as previously described (Figure 3A) to overexpress A1 with the ResA1 gene or A2. The transduced cells are referred to as SKMCs-ResA1 and SKMCs-A2, respectively. SKMCs that overexpressed mCh only (SKMCs-mCh) were also produced as a control. Fluorescent microscopy indicated that mCh was present in all visible SKMCs (supplementary Figure 1).The levels of A1 and A2 mRNA from each of the SKMCs were measured using paralog specific primers in RT-qPCR and this was normalised to the level of GAPDH mRNA. The level of A1 mRNA was approximately 1000-fold higher than A2 in primary human SKMCs (supplementary Figure 2), and increased 3-fold in SKMC-A1 where A1 gene was transduced, whereas SKMC-A2 cells expressed approximately 500-fold higher levels of A2 mRNA after transduction.

The HIV-1 reverse transcription in SKMC was examined as previously described for HEK293T cells. In parallel samples, the infections were incubated for 24 h before a cell lysate was made for detection of firefly luciferase, which reports on successful infection and gene expression by integrated proviral DNA. The qPCR results showed that HIV-1 early DNA was not significantly different between each cellular condition (Figure 5A). However late DNA was significantly increased in SKMCs-ResA1 cells (Figure 5B) compared to controls. This difference resulted in increased reverse transcription efficiency in HIV-1 infected SKMC-ResA1 cells compared to all other SKMCs tested (Figure 5C). Although there was 500 fold more A2 mRNA in SKMCs-A2 cells, there was no significant change in HIV-1 reverse transcription. This data was mirrored by luciferase expression in HIV-1 infected SKMCs, SKMCs-mCh, SKMCs-ResA1 and SKMCs-A2, where luciferase levels were highest in SKMCs-ResA1 cells ($p<0.05$, Figure 5D). Correlation analysis

showed that the reverse transcription efficiency is highly correlated with the level of A1 (r^2=0.832) , but not A2 mRNA (r^2=0.024) in this SKMC culture system (Supplementary Figure 2). The results confirm the data from HEK293T cells, supporting the conclusion that the A1 paralog has superior ability to support HIV-1 reverse transcription and promotes viral infectivity compared to the A2 paralog.

3. Discussion

Evidence that eEF1A plays important roles in the replication of different RNA viruses is growing (reviewed in Li et al., 2013). For example, investigators have reported interaction between eEF1A and the RNA polymerases of various RNA viruses that facilitates their replication (Li et al., 2013). However, most studies have been performed with various transformed cell lines that express A1 and often some level of A2 (Acel et al., 1998; Carr et al., 2008; Qanungo et al., 2004), where the relative ratio of the two paralogs expressed by different cell lines is not well documented. Our previous analysis indicated that HEK293T cells used in this study primarily express A1 as determined by siRNA knockdown experiments that specifically targeted A1 (Warren et al., 2012). Our previous studies demonstrated that A1 interacts with HIV-1 RT and that siRNA down-regulation of A1 in cells subsequently infected with HIV-1 significantly decreased their reverse transcription (Li et al., 2015b; Warren et al., 2012). We believe the same is true for Jurkat cells, where our mass spectrometry analysis identified the A1 paralog, but not the A2 paralog, as being in the Jurkat cell lysate fraction that stimulated reverse transcription (Warren et al., 2012). Here we compared interaction of A1 and A2 with HIV-1 RT and evaluated their ability to support HIV-1 reverse transcription.

We observed that IP of A1 results in much higher amounts of co-IP RT compared to IP of A2. The BLI experiments were performed using highly purified mouse liver or muscle to obtain A1 or A2, respectively, where RT was immobilized on a biosensor in a low ionic strength buffer. In this

case, the K_D measured for the RT:A1 and RT:A2 interactions were similar, 1.2 nM and 2.3 nM respectively, and close to the K_D measured in a previous study that used commercial FLAG-tagged A1, 3.75 nM (Li et al., 2015b). However the k_a and k_d values for A1 and A2 interactions with RT were remarkably dissimilar. The kinetic experiments showed rapid association and dissociation of A2 to RT compared to A1, where the association rate was 3-fold faster and dissociation rate of the eEF1A2:RT complex was 6-fold faster. This kinetic change was reminiscent of the interaction between RT and A1 when a single point mutation in RT, E300R, which had poor binding to eEF1A by co-IP and had increased dissociation rate with eEF1A in BLI while the association rate was unchanged (Rawle et al., 2018). This may suggest that a stable RT:eEF1A1 interaction which dissociates slowly is more important than the association. The binding kinetics profiles suggest that different mechanisms regulate interaction of the two eEF1A paralogs with RT.

The RT:eEF1A1 interaction is important for HIV-1 reverse transcription (Li et al., 2015b; Warren et al., 2012) as demonstrated in our recent report that the E300R mutation in RT disrupts the RT:eEF1A interaction and results in a significant decrease of HIV-1 reverse transcription efficiency and defective replication (Rawle et al., 2018). We assessed the efficiency of HIV-1 reverse transcription in HEK293T cells where levels of each eEF1A paralog were modulated. In repeated experiments we observed a statistically significant effect on late, but not on early, DNA synthesis when the endogenous A1 was downregulated by over 80%; which agreed with our previous report (Warren et al., 2012). Overexpression of exogenous A1, but not A2 restored HIV-1 late DNA synthesis. In all experiments, we noted a slight negative effect of A2 overexpression on late DNA levels in HEK293T cells with control siRNA, which was not observed when A1 was overexpressed or in A2 overexpression in $siRNA_{A1}$ cells. We speculate that a competition between exogenous A2 and endogenous A1 may account for this small effect. The results revealed that HEK293T cells predominantly express A1 protein, but also express A2 at very low levels as determined by A2 mRNA analysis. The level of A1 mRNA, not A2 mRNA, correlated with the HIV-1 reverse

transcription efficiency in HEK293T cells and SKMCs, providing strong support to the finding that A1, not A2, is important for HIV-1 reverse transcription.

The A1 and A2 paralogs share a canonical activity in protein synthesis (Kahns et al., 1998), but they are expressed in distinctly different tissues. Analysis shows that A2 is expressed predominantly in terminally differentiated muscle and neurons while A1 is ubiquitously expressed in nearly all other tissues. The different non-canonical functions of A1 and A2 may explain the why the expression of genes encoding two eEF1A paralogs with such a high amino acid identity and similarity are differentially regulated in different tissues (Soares and Abbott, 2013). For example, A1 has reported pro-apoptotic activity while A2 has anti-apoptotic effects on cells (Hotokezaka et al., 2002). Further emerging evidence that the two eEF1A paralogs have key structural variations, mainly in surface clusters where differences in post-translational modifications (including acetylation, phosphorylation, S-nitrosylation and ubiquitination) and hydrophobic properties, may underlie their ability to undertake their non-canonical cellular activities (Soares and Abbott, 2013; Soares et al., 2009; Timchenko et al., 2013). For example, a recent paper reported that A1, but not A2, can bind with Ca^{2+} calmodulin and that this interaction affects their differences in actin binding properties (Novosylna et al., 2017). Also, evidence that inappropriate expression of A2 in cells which normally only express A1 plays a role in tumorigenesis suggests that the two eEF1A paralogs participate in fundamentally different interactions in the cellular proteome and therefore take on unique functional and expression profiles (Abbas et al., 2012; Abbas et al., 2015). These differences in regulation of cellular functions may also impact on HIV-1 reverse transcription efficiency. For example, actin is involved in uncoating and reverse transcription (Bukrinskaya et al., 1998), and differential regulation of actin by A1 or A2 may indirectly affect reverse transcription, as we recently reported with RSV replication (Snape et al., 2018).

In conclusion, the A1 paralog binds HIV-1 RT with more stability than the A2 paralog, and only the A1 paralog correlated with reverse transcription efficiency. Therefore, the A1 paralog, but

not the A2 paralog, is important for HIV-1 infection. HIV-1 replicates in various human cells, including $CD4^+$ T cells and macrophages, and the CD4 cell surface receptor is a main factor determining cellular cytotropism. However, CD4 negative and A1 paralog dominant epithelial cells of the liver, kidney, and in mammary epithelial cells of HIV-1 infected women are reported to support HIV-1 replication (Kandathil et al., 2016). Alternatively there are controversial reports of HIV-1 infection of neurons and, to our knowledge, no reports of HIV-1 in muscle cells, which both only express A2 (Balinang et al., 2017; Canto-Nogues et al., 2005). The expression profiles of A1 and A2 paralogs of eEF1A may have broad implications in understanding replication of HIV-1 and other viruses, and cytotropism of these viruses.

4. Materials and methods

4.1. Cells and virus culture. HEK293T cells were grown in Dulbecco's modified Eagle's medium supplemented with 10% heat-inactivated fetal bovine serum, penicillin (50 I.U./ml)-streptomycin (50 µg/ml). The human skeletal muscle cells were bought from Lonza Walkersville (USA) and cultured in the growth medium as per manufacturer instructions. Differentiation of myotubes was achieved by replacing growth medium with DMEM-F12 (Lonza, USA) supplemented with 2% horse serum (Sigma, USA). All cell lines were incubated at 37°C in 5% CO_2. The stock of VSV-G pseudotyped $HIV\text{-}1_{NL4\text{-}3}$ or $HIV\text{-}1_{pNL4\text{-}3.Luc.R\text{-}E}$ were generated by co-transfection of a proviral DNA plasmid and VSV-G plasmid into HEK293T cells using Lipofectamine 2000 (Invitrogen, Carlsbad, CA) according to the manufacturer's recommendations. Cell culture supernatants were collected at 48 h post-transfection and centrifuged (200 × *g*, 10 min), and the supernatant was filtered (0.45 µm) and stored in 1 ml aliquots at −80°C.

4.2. Co-immunoprecipitation (Co-IP) . Co-IP was performed as elsewhere described (Warren et al., 2012). Briefly, HEK293T cells were co-transfected with plasmids to express HIV RT-V5 and

over-express eEF1A1-flag or eEF1A2-flag. The cells were lysed at 24 h post-transfection in S100 buffer (10 mM Tris, pH 7.4, 1.5 mM $MgCl_2$, 10 mM KCl, 1× complete protease inhibitor cocktail [Roche], and 0.5 mM β-mercaptoethanol) using a Dounce homogenizer. The lysate was cleared by centrifugation in a microfuge (4°C, 20,000 x *g*, 10 min). The supernatant was incubated with anti-flag rabbit antibody coupled Dynabeads Protein G (Invitrogen, USA) for 2 h at 4°C. The immunoprecipitate was washed three times with S100 buffer plus 0.3% of Triton-x100 followed by western blot analysis using anti-V5 mouse antibody.

4.3. Purification of eEF1A1 and eEF1A2 from mouse tissue. A1 and A2 were purified from adult mouse liver and skeletal muscle respectively using two consecutive ion-exchange column-chromatography steps according to a published method (Yaremchuk et al., 2012). The approval to obtain mouse tissue used in the experiment was provided by QIMR Berghofer Medical Research Institute Animal Ethics Committee. Briefly, 10 g of mouse liver or skeletal muscle was homogenized in 20 ml buffer A (30 mM potassium phosphate pH 7.5, 1 m*M* $MgCl_2$, 15% glycerol, 6 mM β-mercaptoethanol supplemented with 1 mM PMSF) using a tissue grinder. After 40 min of centrifugation at 12,000 × *g*, the supernatant was filtered through four layers of sterile gauze to remove fat. The clear supernatant was loaded onto a DEAE-cellulose column (GE Healthcare) previously equilibrated with buffer A. Unbound proteins were collected and loaded directly onto an SP-Sepharose column (GE Healthcare) equilibrated with buffer *A*. The column was extensively washed with buffer A containing 100 mM KCl until the OD at 280 nm reached the baseline. eEF1A1 and eEF1A2 were eluted from the column with 5 column volume of 200 mM KCl in buffer A and dialyzed against storage buffer (25 mM potassium phosphate pH 7.5, 1 mM $MgCl_2$, 25% glycerol, 2 mM DTT). The presence and purity of eEF1A1 and eEF1A2 were examined by SDS–PAGE followed with Coomassie blue staining and western blot using anti-eEF1A1 and anti-eEF1A2 antibodies.

4.4. BLI assay. The purified recombinant 6×His-tagged HIV-1 RT p51/ p66 (gift from Stuart LeGrice, Duane Grandgenett) were biotinylated using EZ-Link Sulfo-NHS-Biotin following the manufacturer's instructions (Pierce Biotechnology, IL, USA) and immobilized onto OctetRed system streptavidin-coated biosensors (Pall ForteBio, CA, USA). A standard kinetic buffer (1 mM phosphate, 15 mM NaCl, 0.002% Tween-20 and 0.1 mg/ml gelatine) was used in all experiments unless noted. The association (k_a) of the two proteins was measured by incubating ligand biosensors (biotinylated protein) into kinetic buffer containing protein (analyte) with 1000 rpm shaking in the OctetRed system. Concentrations of analyte ranging from 90 nM to 10 nM were assayed. The dissociation (k_d) was determined by moving the ligand biosensor from kinetic buffer containing analyte to the standard kinetic buffer.

4.5. Plasmids. For expression of HIV-1 RT p51 in cells, the coding DNA sequences were amplified from pHGPsyn construct (Wagner et al., 2000), which contains a codon optimized Gag-Pol sequence, and was inserted into pDONR vector using Gateway system (Invitrogen, USA) by a BP recombination reaction. The inserts were then transferred into destination mammalian expression vectors that contain V5 tags by LR recombination reactions. The same strategy was used to construct A1 and A2 expressing plasmid and the proteins were fused with a FLAG tag**.** The cDNA templates were obtained from PlasmID Repository (Harvard).

A1 cDNA sequence was modified to be resistant to siRNA SASI_Hs02_00331772 by mutation of the original A1 cDNA. The modified eEF1A1 (Res-A1) and A2 DNA fragments were excised with *Nhe*I and *Eco*RI and inserted into a pSicoR-EF1a vector (Addgene, Cambridge, MA) at these restriction enzyme sites (Jin et al., 2016) to give the pSicoR-Res-A1 and pSicoR-A2 vectors.

4.6. siRNA treatment. siRNA (Sigma-Aldrich) targeting A1 (siRNA ID: SASI_Hs02_00331772) and control siRNA (SIC001) were applied to HEK293T cells by large-scale reverse transfection using Lipofectamine RNAiMAX according to the manufacturer's instructions (Invitrogen).

4.7. VLP production and transduction. VLPs that convey Re-A1 or A2 were produced by co-transfecting 3 µg of pSicoR-Res-A1 or pSicoR-A2 with 10 µg of plasmid pCMVΔR8.91 and 3 µg of pCMV-VSV-G into HEK293T cells with X-tremeGENE HP DNA transfection reagent (Roche Diagnostics GmbH, Mannheim, Germany) in accordance with the manufacturer's protocol. The cell medium was replaced at 24 h post-transfection. VLPs were harvested by filtration with a sterile 0.2-µm syringe filter (Sartorius Stedim Biotech GmbH, Göttingen, Germany) at 48 h post transfection. The concentration of VLPs was quantified with a RETROtek HIV-1 CAp24 antigen ELISA (Zeptometrix, USA). For transduction, Res-A1 or A2 VLPs were incubated with HEK293T cells in the presence of 8 µg/ml of hexadimethrine bromide (Sigma-Aldrich) and the positive cells were sorted with a MoFlo High Speed Cell Sorter (Beckman Coulter, Pasadena, CA) at 3 day post-transduction.

4.8. Virus infection, DNA extraction and analysis of reverse transcription DNA synthesis.

HIV-$1_{NL4.3}$ virus stock was treated with DNase I at 37 °C for 30 min to remove any DNA contamination prior to adding to cells. HEK293T cells were incubated with HIV-$1_{NL4.3}$ VSV-G pseudotyped virus in presence of 8 µg/ml polybrene at 4°C for 2 h and then 37 °C for 4 h. For SKMCs infection, HIV-$1_{pNL4\text{-}3.Luc.R\text{-}E}$ VSV G pseudotyped virus was used and the infection was performed with centrifugation at 1,200 × g, 16 °C for 2 h and then 37 °C for 4 h. The cells were then washed three times with 0.1 mM EDTA PBS, and lysed using Glo Lysis Buffer (Promega). The lysate was centrifuged (20,000 × *g*, 10 min) and the supernatant was extracted once with an equal volume of phenol:chloroform:isoamyl alcohol (25:24:1) and once with chloroform. The extracts were ethanol precipitated, washed with 70% (vol/vol) ethanol, and resuspended in 0.1 mM EDTA. The early and late HIV-1 reverse transcription products were analyzed by quantitative PCR using specific primers as elsewhere described (Warrilow et al., 2008) .

4.9. RNA extraction and A1, A2 paralog specific RT-qPCR. RNA extraction was performed using TRIzol reagent (Invitrogen, USA) following the manufacturer's instructions. Reverse transcription was carried out using random primers and superscript III reverse transcriptase (Invitrogen, USA). A1 and A2 paralog specific detection is achieved by using specific primers in qPCR. The primer sequences for A1 paralog are GACCAGCAAGTACTATG (forward) and CCAAGCTTCAAATTCACCA (reverse). The sequences of primers for A2 paralog are GACCACCAAGTACTACA (forward) and ATGCCCGCCTCGAACTCG. The cellular gene GAPDH was used as internal controls.

4.10. Statistical analysis. Statistical analyses were performed using a student's unpaired T-test with Welch's correction for least three independent experiments or measurements. Statistical significance was set at $p < 0.05$. The correlation analysis was performed using Graphpad software. The correlation coefficient, $r^2 = 1$ indicating a perfect correlation and $r^2 = 0$ means the two variables do not correlate at all.

Abbreviations

HIV-1: human immunodeficiency virus type 1; eEF1A: eukaryotic translation elongation factor 1A; eEF1A1: eukaryotic translation elongation factor 1A paralog 1; eEF1A:2 eukaryotic translation elongation factor 1A paralog 2; RT: reverse transcription; BLI: biolayer interferometry; SKMC: Primary human skeletal muscle cells**;** VLP: virus like particles

Acknowledgments

This research was supported by a project grant to DH and DL (NHMRC 1080465). The following reagent was obtained through the NIH AIDS Reagent Program, Division of AIDS, NIAID, NIH: pNL4-3.Luc.R–.E– from Dr. Nathaniel Landau.

Competing interests

The authors declare no competing interests exist.

Consent for publication

Not applicable

Ethics approval and consent to participate

No human subjects were used in this study**.**

Funding

This work was supported by the Australian National Health and Medical Research Council (NHMRC) project grant 1080465. Z.L. was supported by a grant of Science and Technology Program - International Cooperation Program (2013ZYH193), Ningxia, China and a grant of Ningxia Key Research and Development Program (2018BEG03065), Ningxia, China.

Figure legends

Fig 1. The A1 paralog of eEF1A binds RT stronger than the A2 paralog by co-IP in HEK293T cells. (A-C) The pDEST-HIV-RTp51-v5 expression plasmids were transfected alone or co-transfected with pDEST-A1-FLAG or pDEST-A2-FLAG into HEK293T cells. A cell lysate was made 24 h post-transfection and analyzed by western blot. RT-v5, or A1-FLAG and A2-FLAG were detected by western blot using anti-V5 or anti-FLAG antibodies, respectively. An anti-β-tubulin antibody was used to detect β-tubulin. Co-IP assays were performed using anti-FLAG antibody labeled beads. The beads were washed in buffer and the level of RT (D) or A1-FLAG and A2-FLAG (E) in IP product was detected by western blot using anti-V5 or anti-FLAG antibodies as shown. The experiment was performed three times with similar results. A representative experiment is shown. The relative RT signal was quantified using ImageJ software and normalized to the FLAG (A1 and A2) signal, and presented as mean of three separate western blot results (F).

Fig 2. **The interaction of RT with purified A1 and A2 show distinct binding kinetics.** (A) The purified A1 from mouse liver and A2 from mouse muscle were analyzed by SDS-PAGE and visualized with Coomassie brilliant blue stain. (B) 100 and 400 ng of A1 and A2 proteins were examined by western blot using anti-eEF1A2 and anti-eEF1A antibodies. (C) The total RNA was extracted from mouse liver and skeletal muscle tissue followed by RT using random primer and qPCR using A1 and A2 specific primers. The level of RNA in each tissue is presented as the mean value of repeated PCR reactions. (D) Distinct binding kinetics observed for A1 and A2 interaction with HIV-1 RT in biolayer interferometry assays. Biotinylated HIV RT was immobilized on streptavidin biosensors and incubated with 90, 30 and 10 nM of purified A1 or A2 protein analytes and real-time binding was measured using the Octet RED system (Li et al., 2015b).

Fig 3. Exogenously expressed ResA1, but not A2, restores reverse transcription efficiency in A1 down-regulated cells. (A) The lentiviral vector pScioR-EF1α was used to deliver mCh-T2A-ResA1 or mCh-T2A-A2 to HEK 293T cells by transduction. Res-A1 has the same amino acid sequence as endogenous A1 but is resistant to $siRNA_{A1}$. The T2A ribosomal skipping sequence permits independent translation of mCh-T2A and Res-A1 or A2. Due to T2A skipping, exogenous ResA1 and A2 proteins have an additional proline residue on the N-terminus. The mCh-T2A positive cells were purified by FACS. (B) Parental HEK 293T cells (cells only sample) or HEK 293T cells over expressing exogenous ResA1 or A2 were treated with $siRNA_{A1}$ that targets endogenous A1 mRNA, or a $siRNA_C$ as a control as indicated. At 48 h post-treatment, a cell lysate was made and the level of eEF1A in the samples was detected by western blot using an anti-eEF1A polyclonal antibody. This includes endogenous A1 and exogenously expressed ResA1 or A2 (upper panel). A western blot of the same lysate for β-tubulin is shown (lower panel). The signal was quantified using ImageJ and normalised to the signal of the control siRNA sample. (C and D) The cells were infected with HIV-$1_{pNL4\text{-}3.Luc.R\text{-}E}$ pseudotyped with VSV-G by incubation with the cells for 2 h at 4 °C to allow virus attachment, and then at 37 °C for 4 h to initiate virus entry and reverse transcription. Cell lysates

were made from the infected cells and the levels of HIV-1 early and late reverse transcribed DNA in each sample were measured by qPCR as previous described (Warren et al., 2012). (E) The reverse transcription efficiency was calculated as the ratio of late DNA to early DNA as a percentage. The mean of at least three experiments and the standard deviations are shown. P values of comparisons that had statistically significant differences are shown.

Fig 4. HIV-1 reverse transcription efficiency correlated with the level of eEF1A1, not eEF1A2 in HEK293T cells. A1, A2 and GAPDH mRNA copied were measured by RT-qPCR from RNA extracted from cells. The HIV-1 reverse transcription early and late DNA products were measured by qPCR from cell lysates prepared at 4 h post-infection with HIV. The A1 or A2 mRNA copy number were normalized to GAPDH mRNA. RT efficiency was calculated by copy number of late DNA/copy number of early DNA. The data is presented as mean ± SD from three independent experiments. Correlation analysis was performed between the relative levels of A1 (A) or A2 (B) with the RT efficiencies. The value of r^2 approaching 1 indicates high correlation, while approaching 0 indicates low correlation.

Fig 5. Overexpression of Res-A1 increases HIV-1 reverse transcription efficiency in SKMCs. Untreated SKMCs, SKMCs expressing Res-A1 (SKMCs-Res-A1), A2 (SKMCs-A2) or mCh-T2A (SKMCs-mCh) were infected with HIV-$1_{pNL4\text{-}3.Luc.R\text{-}E}$ pseudotyped with VSV-G at 1,200 × g at 16°C for 2 h, and then incubated at 37°C for 4 h or 24 h. The 4 h sample cell lysates were prepared for (A) early and (B) late HIV-1 DNA detection by qPCR, and (C) is the ratio of late/early DNA. (D) SKMCs expressing mCh, Res-A1 or A2 were infected with HIV-$1_{pNL4\text{-}3.Luc.R\text{-}E}$ pseudotyped with VSV-G for 48 h and luciferase in cell lysates were measured using firefly luciferase. The mean of at least three experiments and the standard deviations are shown. P values for observations that had statistically significant differences are shown.

References

Abbas, W., Khan, K.A., Tripathy, M.K., Dichamp, I., Keita, M., Rohr, O., Herbein, G., 2012. Inhibition of ER stress-mediated apoptosis in macrophages by nuclear-cytoplasmic relocalization of eEF1A by the HIV-1 Nef protein. Cell Death Dis 3, e292.

Abbas, W., Kumar, A., Herbein, G., 2015. The eEF1A Proteins: At the Crossroads of Oncogenesis, Apoptosis, and Viral Infections. Front Oncol 5, 75.

Acel, A., Udashkin, B.E., Wainberg, M.A., Faust, E.A., 1998. Efficient gap repair catalyzed in vitro by an intrinsic DNA polymerase activity of human immunodeficiency virus type 1 integrase. J Virol 72, 2062-2071.

Balinang, J.M., Masvekar, R.R., Hauser, K.F., Knapp, P.E., 2017. Productive infection of human neural progenitor cells by R5 tropic HIV-1: opiate co-exposure heightens infectivity and functional vulnerability. AIDS 31, 753-764.

Bissel, S.J., Wiley, C.A., 2004. Human immunodeficiency virus infection of the brain: pitfalls in evaluating infected/affected cell populations. Brain Pathol 14, 97-108.

Bukrinskaya, A., Brichacek, B., Mann, A., Stevenson, M., 1998. Establishment of a functional human immunodeficiency virus type 1 (HIV-1) reverse transcription complex involves the cytoskeleton. J Exp Med 188, 2113-2125.

Canto-Nogues, C., Sanchez-Ramon, S., Alvarez, S., Lacruz, C., Munoz-Fernandez, M.A., 2005. HIV-1 infection of neurons might account for progressive HIV-1-associated encephalopathy in children. J Mol Neurosci 27, 79-89.

Carr, J.M., Coolen, C., Davis, A.J., Burrell, C.J., Li, P., 2008. Human immunodeficiency virus 1 (HIV-1) virion infectivity factor (Vif) is part of reverse transcription complexes and acts as an accessory factor for reverse transcription. Virology 372, 147-156.

Chang, R., Wang, E., 2007. Mouse translation elongation factor eEF1A-2 interacts with Prdx-I to protect cells against apoptotic death induced by oxidative stress. J Cell Biochem 100, 267-278.

Cimarelli, A., Luban, J., 1999. Translation elongation factor 1-alpha interacts specifically with the human immunodeficiency virus type 1 Gag polyprotein. J Virol 73, 5388-5401.

Francis, A.C., Melikyan, G.B., 2018. Single HIV-1 Imaging Reveals Progression of Infection through CA-Dependent Steps of Docking at the Nuclear Pore, Uncoating, and Nuclear Transport. Cell Host Microbe 23, 536-548 e536.

Gonen, H., Smith, C.E., Siegel, N.R., Kahana, C., Merrick, W.C., Chakraburtty, K., Schwartz, A.L., Ciechanover, A., 1994. Protein synthesis elongation factor EF-1 alpha is essential for ubiquitin-dependent degradation of certain N alpha-acetylated proteins and may be substituted for by the bacterial elongation factor EF-Tu. Proc Natl Acad Sci U S A 91, 7648-7652.

Hassan, M.K., Kumar, D., Naik, M., Dixit, M., 2018. The expression profile and prognostic significance of eukaryotic translation elongation factors in different cancers. PLoS One 13, e0191377.

Herschhorn, A., Oz-Gleenberg, I., Hizi, A., 2008. Quantitative analysis of the interactions between HIV-1 integrase and retroviral reverse transcriptases. Biochem J 412, 163-170.

Hotokezaka, Y., Tobben, U., Hotokezaka, H., Van Leyen, K., Beatrix, B., Smith, D.H., Nakamura, T., Wiedmann, M., 2002. Interaction of the eukaryotic elongation factor 1A with newly synthesized polypeptides. J Biol Chem 277, 18545-18551.

Jin, H., Li, D., Sivakumaran, H., Lor, M., Rustanti, L., Cloonan, N., Wani, S., Harrich, D., 2016. Shutdown of HIV-1 Transcription in T Cells by Nullbasic, a Mutant Tat Protein. MBio 7.

Kahns, S., Lund, A., Kristensen, P., Knudsen, C.R., Clark, B.F., Cavallius, J., Merrick, W.C., 1998. The elongation factor 1 A-2 isoform from rabbit: cloning of the cDNA and characterization of the protein. Nucleic Acids Res 26, 1884-1890.

Kandathil, A.J., Sugawara, S., Balagopal, A., 2016. Are T cells the only HIV-1 reservoir? Retrovirology 13, 86.

Khacho, M., Mekhail, K., Pilon-Larose, K., Pause, A., Cote, J., Lee, S., 2008. eEF1A is a novel component of the mammalian nuclear protein export machinery. Mol Biol Cell 19, 5296-5308.

Kim, S., Coulombe, P.A., 2010. Emerging role for the cytoskeleton as an organizer and regulator of translation. Nat Rev Mol Cell Biol 11, 75-81.

Kohler, A., Hurt, E., 2007. Exporting RNA from the nucleus to the cytoplasm. Nat Rev Mol Cell Biol 8, 761-773.

Li, D., Wei, T., Abbott, C.M., Harrich, D., 2013. The unexpected roles of eukaryotic translation elongation factors in RNA virus replication and pathogenesis. Microbiol Mol Biol Rev 77, 253-266.

Li, D., Wei, T., Jin, H., Rose, A., Wang, R., Lin, M.H., Spann, K., Harrich, D., 2015a. Binding of the eukaryotic translation elongation factor 1A with the 5'UTR of HIV-1 genomic RNA is important for reverse transcription. Virol J 12, 118.

Li, D., Wei, T., Rawle, D.J., Qin, F., Wang, R., Soares, D.C., Jin, H., Sivakumaran, H., Lin, M.H., Spann, K., Abbott, C.M., Harrich, D., 2015b. Specific Interaction between eEF1A and HIV RT Is Critical for HIV-1 Reverse Transcription and a Potential Anti-HIV Target. PLoS Pathog 11, e1005289.

Mamede, J.I., Cianci, G.C., Anderson, M.R., Hope, T.J., 2017. Early cytoplasmic uncoating is associated with infectivity of HIV-1. Proc Natl Acad Sci U S A 114, E7169-E7178.

Mateyak, M.K., Kinzy, T.G., 2010. eEF1A: thinking outside the ribosome. J Biol Chem 285, 21209-21213.

Murthi, A., Shaheen, H.H., Huang, H.Y., Preston, M.A., Lai, T.P., Phizicky, E.M., Hopper, A.K., 2010. Regulation of tRNA bidirectional nuclear-cytoplasmic trafficking in Saccharomyces cerevisiae. Mol Biol Cell 21, 639-649.

Nagy, P.D., 2015. Viral sensing of the subcellular environment regulates the assembly of new viral replicase complexes during the course of infection. J Virol 89, 5196-5199.

Novosylna, O., Doyle, A., Vlasenko, D., Murphy, M., Negrutskii, B., El'skaya, A., 2017. Comparison of the ability of mammalian eEF1A1 and its oncogenic variant eEF1A2 to interact with actin and calmodulin. Biol Chem 398, 113-124.

Qanungo, K.R., Shaji, D., Mathur, M., Banerjee, A.K., 2004. Two RNA polymerase complexes from vesicular stomatitis virus-infected cells that carry out transcription and replication of genome RNA. Proc Natl Acad Sci U S A 101, 5952-5957.

Rawle, D.J., Li, D., Swedberg, J.E., Wang, L., Soares, D.C., Harrich, D., 2018. HIV-1 Uncoating and Reverse Transcription Require eEF1A Binding to Surface-Exposed Acidic Residues of the Reverse Transcriptase Thumb Domain. MBio 9.

Ruest, L.B., Marcotte, R., Wang, E., 2002. Peptide elongation factor eEF1A-2/S1 expression in cultured differentiated myotubes and its protective effect against caspase-3-mediated apoptosis. J Biol Chem 277, 5418-5425.

Schneider, C.A., Rasband, W.S., Eliceiri, K.W., 2012. NIH Image to ImageJ: 25 years of image analysis. Nat Methods 9, 671-675.

Shamovsky, I., Ivannikov, M., Kandel, E.S., Gershon, D., Nudler, E., 2006. RNA-mediated response to heat shock in mammalian cells. Nature 440, 556-560.

Snape, N., Li, D., Wei, T., Jin, H., Lor, M., Rawle, D.J., Spann, K.M., Harrich, D., 2018. The eukaryotic translation elongation factor 1A regulation of actin stress fibers is important for infectious RSV production. Virol J 15, 182.

Soares, D.C., Abbott, C.M., 2013. Highly homologous eEF1A1 and eEF1A2 exhibit differential post-translational modification with significant enrichment around localised sites of sequence variation. Biol Direct 8, 29.

Soares, D.C., Barlow, P.N., Newbery, H.J., Porteous, D.J., Abbott, C.M., 2009. Structural models of human eEF1A1 and eEF1A2 reveal two distinct surface clusters of sequence variation and potential differences in phosphorylation. PLoS One 4, e6315.

Timchenko, A.A., Novosylna, O.V., Prituzhalov, E.A., Kihara, H., El'skaya, A.V., Negrutskii, B.S., Serdyuk, I.N., 2013. Different oligomeric properties and stability of highly homologous A1 and proto-oncogenic A2 variants of mammalian translation elongation factor eEF1. Biochemistry 52, 5345-5353.

Vera, M., Pani, B., Griffiths, L.A., Muchardt, C., Abbott, C.M., Singer, R.H., Nudler, E., 2014. The translation elongation factor eEF1A1 couples transcription to translation during heat shock response. Elife 3, e03164.

Wagner, R., Graf, M., Bieler, K., Wolf, H., Grunwald, T., Foley, P., Uberla, K., 2000. Rev-independent expression of synthetic gag-pol genes of human immunodeficiency virus type 1 and simian immunodeficiency virus: implications for the safety of lentiviral vectors. Hum Gene Ther 11, 2403-2413.

Warren, K., Wei, T., Li, D., Qin, F., Warrilow, D., Lin, M.H., Sivakumaran, H., Apolloni, A., Abbott, C.M., Jones, A., Anderson, J.L., Harrich, D., 2012. Eukaryotic elongation factor 1 complex subunits are critical HIV-1 reverse transcription cofactors. Proc Natl Acad Sci U S A 109, 9587-9592.

Warrilow, D., Meredith, L., Davis, A., Burrell, C., Li, P., Harrich, D., 2008. Cell factors stimulate human immunodeficiency virus type 1 reverse transcription in vitro. J Virol 82, 1425-1437.

Yaremchuk, A., Shalak, V.F., Novosylna, O.V., Negrutskii, B.S., Crepin, T., El'skaya, A.V., Tukalo, M., 2012. Purification, crystallization and preliminary X-ray crystallographic analysis of mammalian translation elongation factor eEF1A2. Acta Crystallogr Sect F Struct Biol Cryst Commun 68, 295-297.

Figure 1

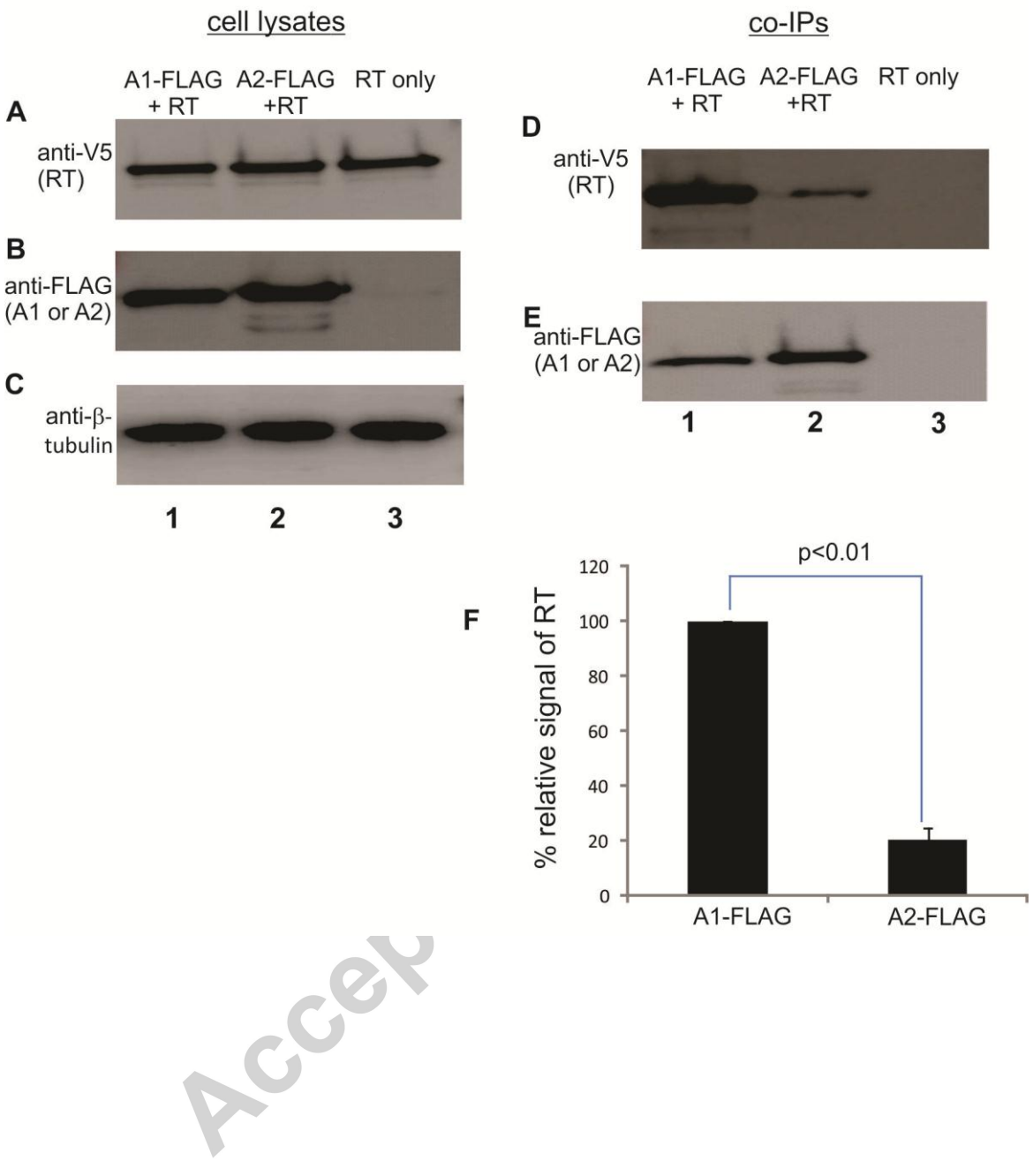

Figure 2

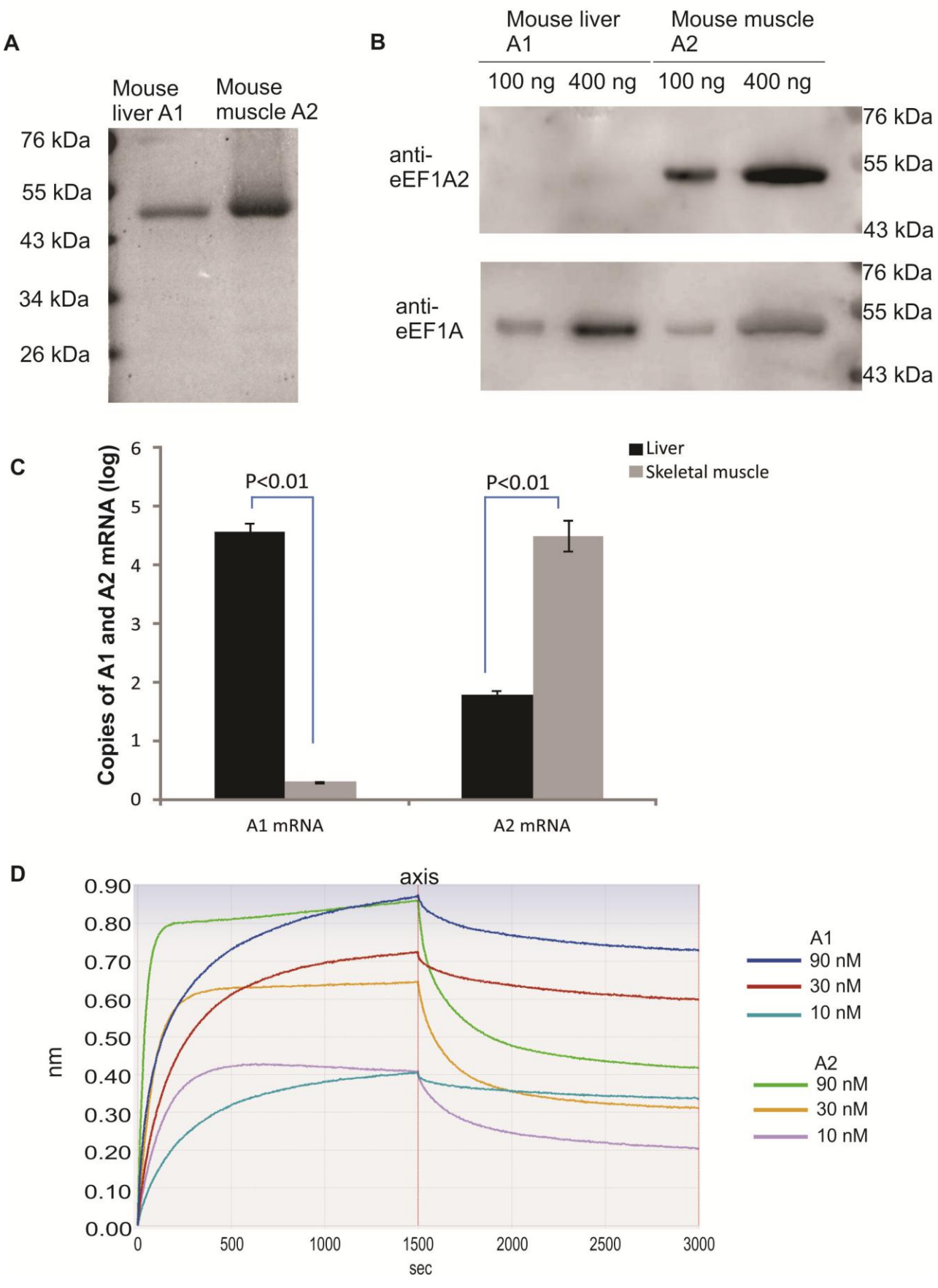
A
Mouse liver A1
Mouse muscle A2
76 kDa
55 kDa
43 kDa
34 kDa
26 kDa
B
Mouse liver A1
Mouse muscle A2
100 ng
400 ng
100 ng
400 ng
anti-eEF1A2
anti-eEF1A
76 kDa
55 kDa
43 kDa
C
Copies of A1 and A2 mRNA (log)
Liver
Skeletal muscle
P<0.01
P<0.01
A1 mRNA
A2 mRNA
D
axis
nm
sec
A1
90 nM
30 nM
10 nM
A2
90 nM
30 nM
10 nM

Figure 3

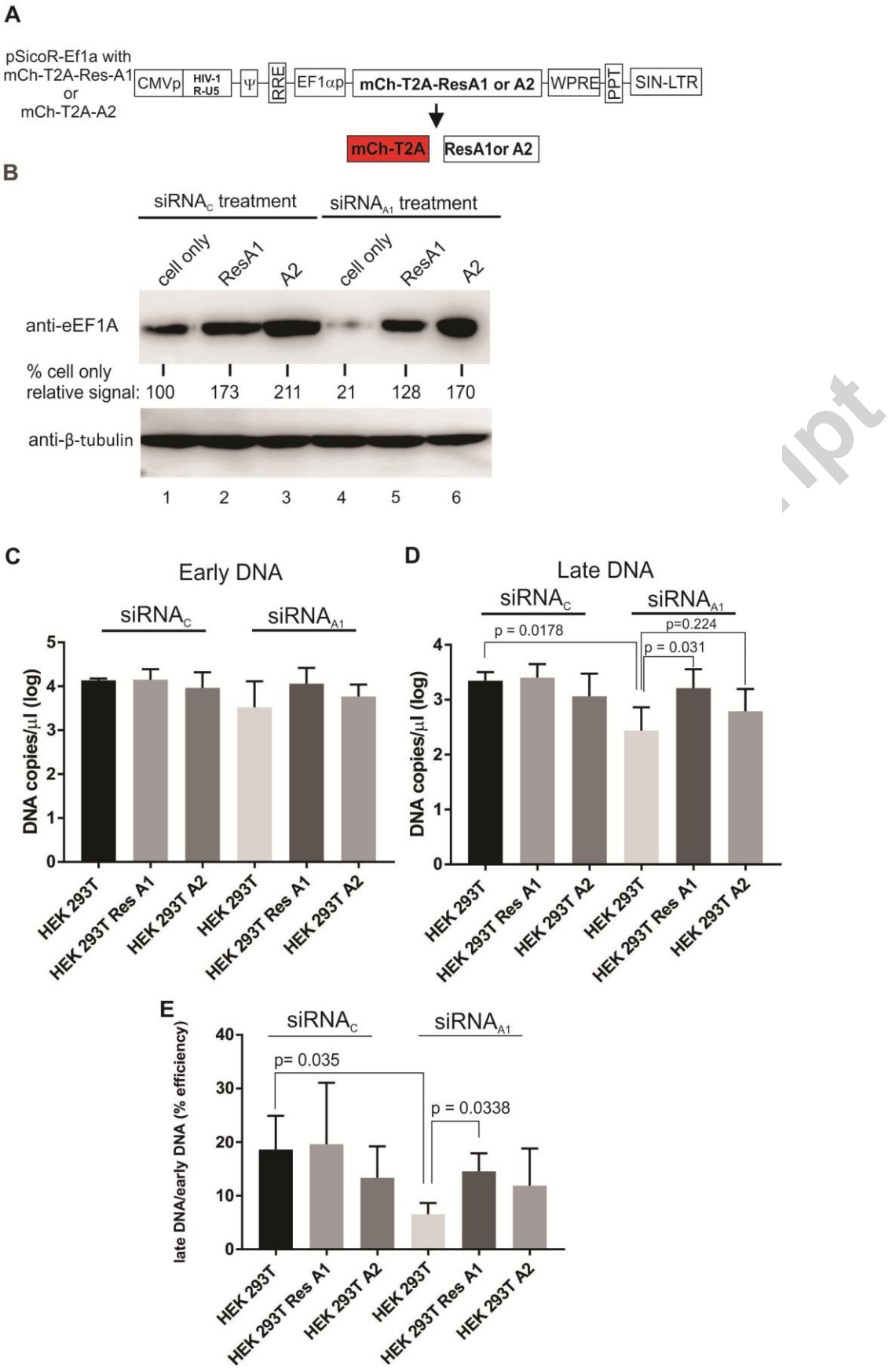
A
pSicoR-Ef1a with mCh-T2A-Res-A1 or mCh-T2A-A2
CMVp
HIV-1 R-U5
Ψ
RRE
EF1αp
mCh-T2A-ResA1 or A2
WPRE
PPT
SIN-LTR
mCh-T2A
ResA1or A2
B
siRNA$_C$ treatment
siRNA$_{A1}$ treatment
cell only
ResA1
A2
cell only
ResA1
A2
anti-eEF1A
% cell only relative signal: 100 173 211 21 128 170
anti-β-tubulin
1 2 3 4 5 6
C
Early DNA
siRNA$_C$
siRNA$_{A1}$
DNA copies/µl (log)
HEK 293T
HEK 293T Res A1
HEK 293T A2
HEK 293T
HEK 293T Res A1
HEK 293T A2
D
Late DNA
siRNA$_C$
siRNA$_{A1}$
p = 0.0178
p=0.224
p = 0.031
DNA copies/µl (log)
HEK 293T
HEK 293T Res A1
HEK 293T A2
HEK 293T
HEK 293T Res A1
HEK 293T A2
E
siRNA$_C$
siRNA$_{A1}$
p= 0.035
p = 0.0338
late DNA/early DNA (% efficiency)
HEK 293T
HEK 293T Res A1
HEK 293T A2
HEK 293T
HEK 293T Res A1
HEK 293T A2

Figure 4

A

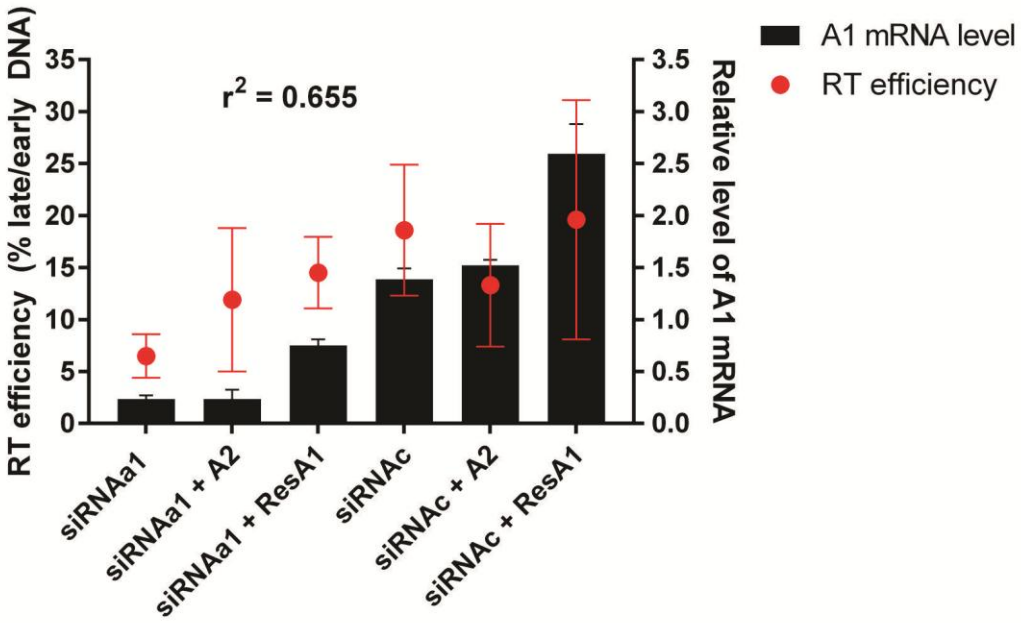
A1 mRNA level
RT efficiency
r^2 = 0.655
RT efficiency (% late/early DNA)
Relative level of A1 mRNA
0
5
10
15
20
25
30
35
0.0
0.5
1.0
1.5
2.0
2.5
3.0
3.5
siRNAa1
siRNAa1 + A2
siRNAa1 + ResA1
siRNAc
siRNAc + A2
siRNAc + ResA1

B

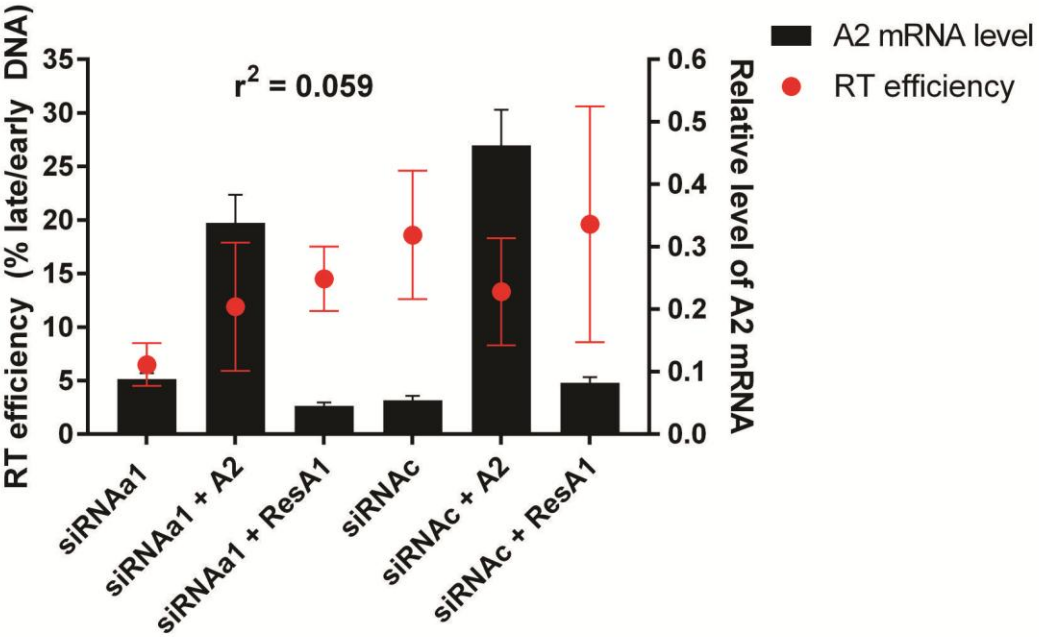
A2 mRNA level
RT efficiency
r^2 = 0.059
RT efficiency (% late/early DNA)
Relative level of A2 mRNA
0
5
10
15
20
25
30
35
0.0
0.1
0.2
0.3
0.4
0.5
0.6
siRNAa1
siRNAa1 + A2
siRNAa1 + ResA1
siRNAc
siRNAc + A2
siRNAc + ResA1

Figure 5

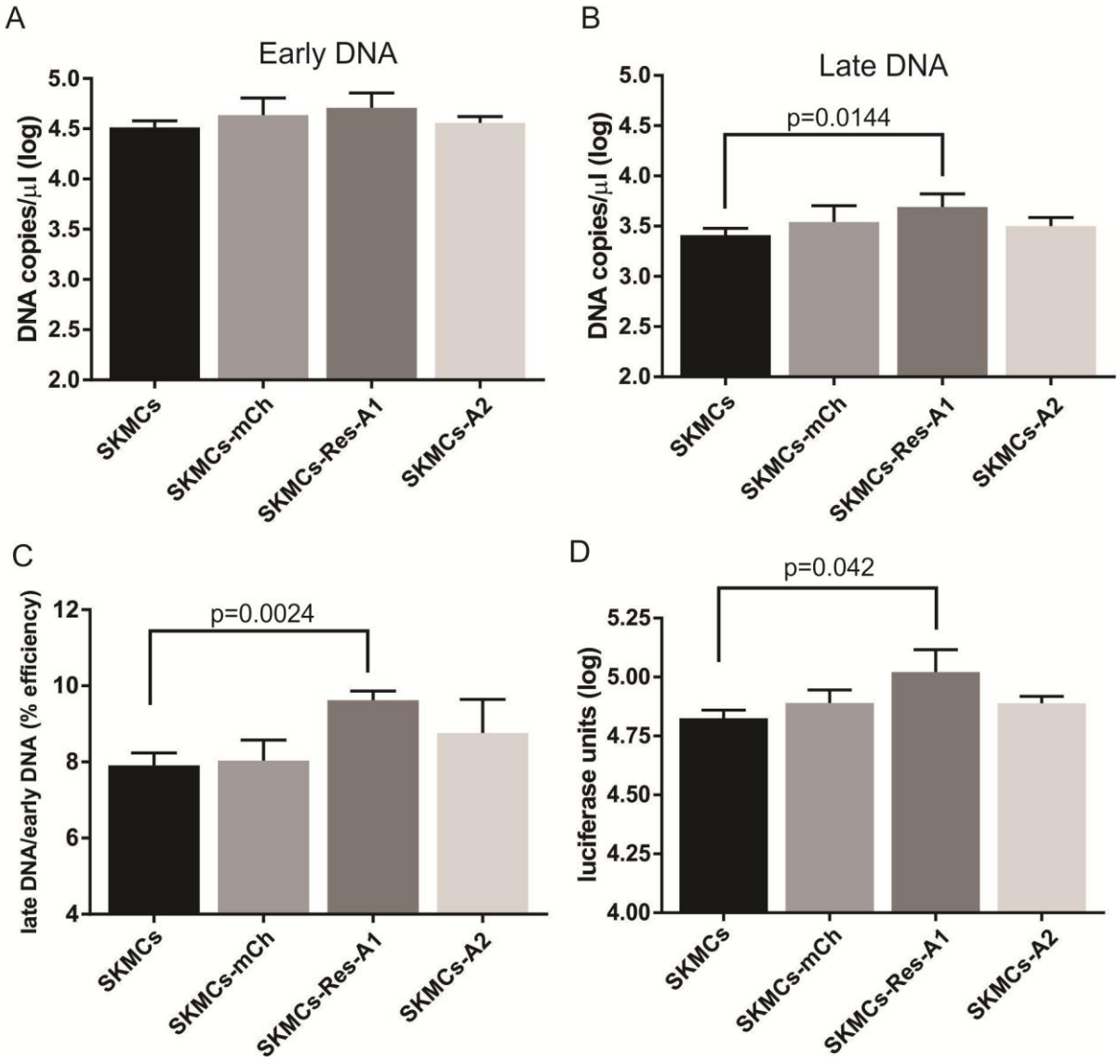
A
Early DNA
DNA copies/μl (log)
5.0
4.5
4.0
3.5
3.0
2.5
2.0
SKMCs
SKMCs-mCh
SKMCs-Res-A1
SKMCs-A2
B
Late DNA
p=0.0144
DNA copies/μl (log)
5.0
4.5
4.0
3.5
3.0
2.5
2.0
SKMCs
SKMCs-mCh
SKMCs-Res-A1
SKMCs-A2
C
p=0.0024
late DNA/early DNA (% efficiency)
12
10
8
6
4
SKMCs
SKMCs-mCh
SKMCs-Res-A1
SKMCs-A2
D
p=0.042
luciferase units (log)
5.25
5.00
4.75
4.50
4.25
4.00
SKMCs
SKMCs-mCh
SKMCs-Res-A1
SKMCs-A2